Advanced Engineering Technology and Application
An International Journal

http://dx.doi.org/10.18576/aeta/050104

Study of Structural and Magnetic Properties of $Mn_{0.8}Zn_{0.2}Fe_2O_4$ Nanoparticles

Nidhi Tendulkar[1], *Suvarna Patil*[1], *Vibhav Kuncalienkar*[1], *Pranav P. Naik*[2], *Mandakini Kundaikar*[1] *and Satish Keluskar*[1,*].

[1] P.E.S.'s Shri Ravi Sitaram Naik College of Arts & Science, Farmagudi, Ponda, Goa, India 403401.
[2] Department of Physics, Goa University, Taleigao Plateau, Goa, India 403206.

Received: 7 Sep. 2015, Revised: 22 Nov. 2015, Accepted: 24 Nov. 2015.
Published online: 1 Jan. 2016.

Abstract: Nanopowder of $Mn_{0.8}Zn_{0.2}Fe_2O_4$ sample was prepared by employing combustion method. Nanocrystalline material obtained at the end of synthesis was subjected to characterization techniques like X-Ray diffraction and Fourier Transform Infrared spectroscopy for structural confirmation. Structural parameters like lattice constant, particle size, X-ray density and bulk density were determined from XRD data. Magnetic parameters like saturation magnetization (MS), remnant magnetization (MR) and Coercivity (HC) were obtained at various temperatures (100K, 150K, 200K, 250K and 300K) using Vibrating Sample Magnetometer to examine the magnetic behavior of the material at various temperatures. Investigations were carried out using Mossbauer spectroscopy at room temperature to divulge structural and magnetic information of the material. Well defined doublet along with magnetic sextets confirms the presence of superparamagnetic nanoparticles. Lower values of isomer shift and quadruple splitting suggest the presence of Fe in +3 oxidation state.

Keywords: Nanopowder, lattice constant, particle size, nanoparticles.

1 Introduction

Compounds with spinel structure belong to a very important group of magnetic materials due to their extensive use in a wide range of applications from low to high permeability devices including electronics, ferrofluid, magnetic drug delivery microwave devices and high density information storage devices [1-4]. These are the materials with general formula of AFe_2O_4 where A can be any divalent transition metal ion. A unit cell contains 32 Oxygen atoms in a cubic close packing with 8 tetrahedral and 16 octahedral occupied sites. The magnetic and electrical properties of these materials depend on the nature and distribution of their cations in these two sites. Manganese Zinc ferrite is known for high saturation, permeability, low hysteresis loss and its high electrical resistivity. In present work we report the results of structural and magnetic investigations carried out on nanocrystalline $Mn_{0.8}Zn_{0.2}Fe_2O_4$ sample synthesized using combustion method.

2 Experimental

2.1 Sample preparation

Ultrafine $Mn_{0.8}Zn_{0.2}Fe_2O_4$ powder was prepared using auto combustion method [5-7]. Metal salts in acetate and nitrate form were taken in stoichometric proportions as raw materials for the sample preparation. The raw materials were mixed with proportionate amount of Nitrilotriacetic acid, used as a complexing agent and Glycene as a fuel for auto combustion. The method adopted is very simple, cost effective and provides an improved particle size distribution.

3 Characterization

X-Ray Diffraction patterns of as prepared MnxZn1-xFe2O4 samples were obtained on Righaku X-Ray diffractometer (λ=1.5418 A). Parameters like lattice constant, particle size and X-Density were calculated from the XRD data obtained on the sample. Magnetic parameters such as saturation magnetization (MS), remnant magnetization (MR) and coercive field (HC) for samples at various temperatures were obtained using Quantum Design's PPMS VersaLab Vibrating Sample Magnetometer (VSM).

Mössbauer spectra of these samples were recorded using conventional Mössbauer spectrometer in constant acceleration mode with Co-57 radioactive source embedded in rhodium matrix of 50 mCi.

*Corresponding author e-mail: shpk@rediffmail.com

© 2016 NSP
Natural Sciences Publishing Cor.

4 Results and Discussion

4.1 X-Ray diffraction

Figure 1 represents the diffraction patterns for $Mn_{0.8}Zn_{0.2}Fe_2O_4$ as prepared sample. The diffraction patterns

Table 1 Structural parameter values obtained from XRD data and mass density for nanocrystalline $Mn_{0.8}Zn_{0.2}Fe_2O_4$.

Sample	Lattice Constant "*a*" (Å)	Particle size "*t*" (nm)	X-ray Denisty "D_x" (g/cc)	MassDensity "D_m"(g/cc)
$Mn_{0.8}Zn_{0.2}Fe_2O_4$	8.4275	53	5.165	6.364

obtained was compared with ICDD card 10-0319 which testifies that sample exhibit a cubic spinel structure. Particle size was obtained from XRD data by employing Sherrer's formula (equation 1) and applying particle strain corrections to FWHM using Williamson Hall plots as shown in Figure 2.

$$t=K\lambda/\beta Cos\theta \quad (1)$$

Where λ is the wave length of X-rays, β is full width at half maximum and K is the Sherrers's constant (K=0.9).

X-ray density of the material was determined using the equation 2 given as;

$$D_x=8M_x/N\,a^3 \quad (2)$$

Where 'N' is Avogadro's number (N=6.0225x10^{23} atoms/mole) and M_x is the molecular weight of the sample and 'a' is lattice constant.

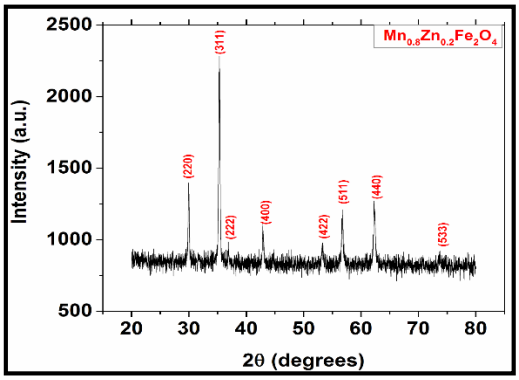

Fig. 1 X-Ray diffraction pattern for $Mn_{0.8}Zn_{0.2}Fe_2O_4$

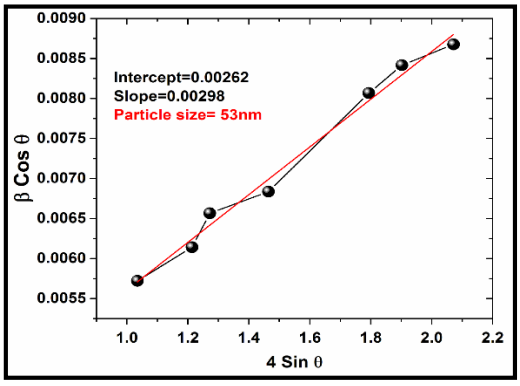

Fig. 2 Williamson Hall plots for as prepared $Mn_{0.8}Zn_{0.2}Fe_2O_4$. Indexed with all spinel peaks

4.2 Fourier Transform Infra-red Spectroscopy

The broad absorption band 559.25cm^{-1} is assigned to M_T -- O --M_O stretching vibration whereas the absorption peak observed at 433.19 cm^{-1} is due to stretching vibration of metal at M_O --O bond and a band at 353.51 cm^{-1} is assigned to M_T -- O bond. Where O is oxygen, M_O is metal in the octahedral site and M_T is metal ion the tetrahedral site. Thus an IR spectrum shown in fig. 3 confirms formation of the required sample [10].

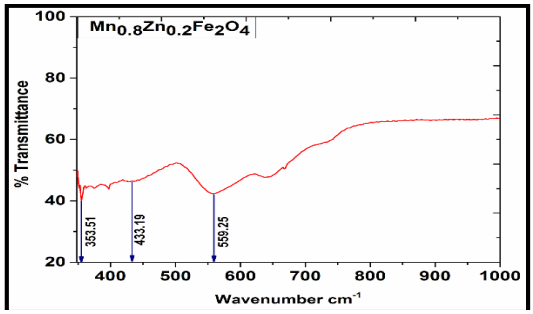

Fig. 3 IR pattern of $Mn_{0.8}Zn_{0.2}Fe_2O_4$

4.3 Magnetic Properties

4.3.1 Vibrating Sample Magnetometer (VSM) measurements

Magnetic properties were measured by the VSM at 300K, 250K, 200K, 150K and100K for the auto-combusted $Mn_{0.8}Zn_{0.2}Fe_2O_4$ powder. The magnetization loops obtained at different temperatures present negligible remenance and hysteresis showing the superparamagnetic nature of the sample as shown in Figure 4.

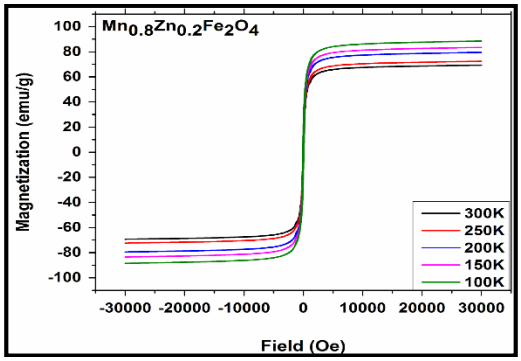

Fig. 4 Hyaterisis curves for $Mn_{0.8}Zn_{0.2}Fe_2O_4$ at different temperatures.

© 2016 NSP
Natural Sciences Publishing Cor.

However saturation magnetization (M_S) was found to increase with reduction in temperature as shown in Figure 5. Remnant magnetization (M_R) and Coercivity (H_C) were also found to increase with reduction in temperature as shown in Figure 6. This enhancement in magnetic parameters can be attributed to surface effects and superparamagnetic nature exhibited by the nanoferrites [11].

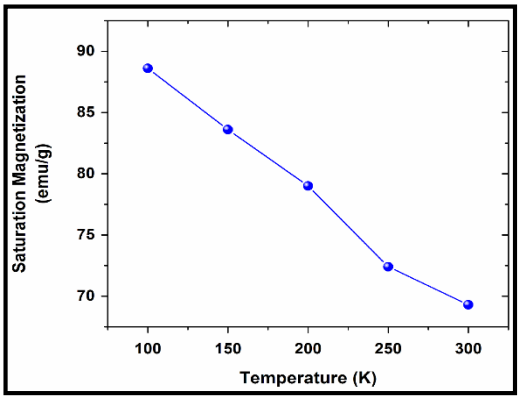

Fig. 5 Saturation magnetization (M_S) variation with temperature

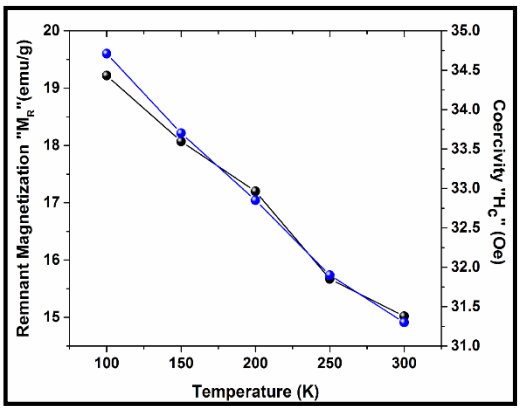

Fig. 6 Remnant magnetization (MR) and coercivity (HC) variation with temperature

4.4 Mössbauer Spectroscopy

Mössbauer spectrum of sample $Mn_{0.8}Zn_{0.2}Fe_2O_4$ was recorded at 300K in the velocity range of -11.5 to 11.5mm/s and is presented in Figure 7. Mössbauer spectrum was fitted by a least square fit program assuming Lorentzian line shapes where the open circles are the experimental data and the solid lines are the fitted data. Mössbauer spectrum was fitted with a doublet and six sextets. This also confirms the ferromagnetic nature of the compound [12]. Out of these six sextets, sextet B corresponds to tetrahedral site Fe ion and sextet A, C, D, E, F represent octahedral site Fe ion. The isomershift (IS), quadrupole splitting (QS) and hyperfine field (Hf) calculated from the fitting of spectra of both as prepared as well as gamma irradiated samples are tabulated in Table 2.

Electrostatic interaction between the charge distribution of the nucleus and s-electrons having finite probability of being found in that region, close to the nucleus results in Isomer shift. Isomer shift for octahedral (B) sites is more than that of the tetrahedral (A) sites due to larger bond length between Fe^{3+}- O in cubic spinel ferrites as compared to that for tetrahedral sites. As a result over lapping of orbitals of Fe^{+3} ions is smaller at octahedral (B) sites and thus, a larger IS is produced indicating a higher s- electron density at B site [13,14].

Non-zero quadrupole splitting arises due to chemical disorder. This produces an electric field gradient (EFG) of varying magnitude, directions, sign and symmetry is produced which results in a distribution in the quadruple shift. In present work paramagnetic doublet appears in the Mossbauer spectrum within the sextet, which can be attributed to interaction of electric field gradient (EFG) with the quadruple moment of ^{57}Fe nucleus and reduction in magnetic interaction between iron ions due to non-magnetic Zn^{+2} ions [15-18].

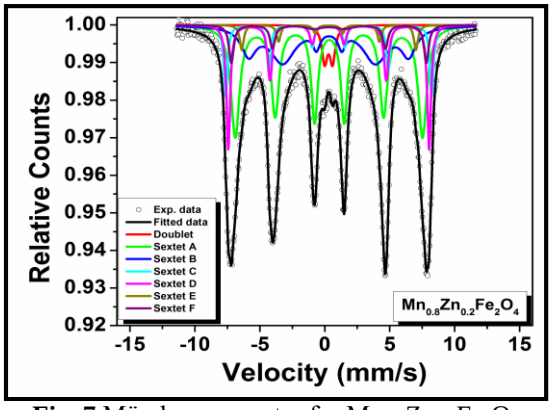

Fig. 7 Mössbauer spectra for $Mn_{0.8}Zn_{0.2}Fe_2O_4$

© 2016 NSP
Natural Sciences Publishing Cor.

Table 2 The isomershift (IS), quadrupole splitting (QS) and hyperfine field (Hf) calculated from the fitting of spectra of both as prepared as well as gamma irradiated samples.

Iron site Spectra	Isomer shift (IS) (mm/s)	Quadrupole splitting (QS) (mm/s)	Hyperfine Field (H_f) (Tesla)	Relative area, R_A (%)
Doublet (S. P.)	0.294± 0.001	0.610±0.001	-	1.4
Sextet (A) (Octa)	0.338±0.012	0.039±0.013	44.69±0.421	39.6
Sextet (B) (Tetra)	0.315±0.066	-0.031±0.007	38.18±1.777	26.8
Sextet (C) (Octa)	0.385±0.0514	0.011±0.002	48.65±0.243	5.5
Sextet (D) (Octa)	0.343±0.0317	0.046±0.013	47.90±0.275	9.9
Sextet (E) (Octa)	0.413± 0.033	0.010±0.003	41.61±0.338	1.9
Sextet (F) (Octa)	0.320±0.003	0.017±0.001	46.54±0.756	14.8

5 Conclusion

Nanocrystalline $Mn_{0.8}Zn_{0.2}Fe_2O_4$ sample was synthesized using combustion synthesis with particle size of approximately 53nm. Lattice constant was found to be 8.427Å. Sample shows a remarkable enhancement in saturation magnetization at lower temperatures along with small but similar alterations in remnant magnetization and coercivity. Samples also exhibit superparamagnetic behavior at all temperatures.

References

[1] Y. Qu, H. Yang, N. Yang, Y. Fan, H. Zhu and G. Zou, Mater. Lett, 60, 3548-3522 (2006).

[2] P. C. Dorsey, P. Lubitz, D. B. Chrisey and J. S. Horwitz, J. Appl. Phys., 85, 6338-6345 (1999).

[3] M. H. Sousa, F. A. Tourinho, J. Phys. Chem. B, 105, 1168-1175 (2001).

[4] F. Mazaleyrat and L. K. Varga, J. Magn. Magn. Mater, 215-216, 253-259 (2000).

[5] D. E. Speliotis, J. Magn. Magn. Mater, 93, 29-35 (1999).

[6] R. B. Tangsali, S. H. Keluskar, G. K. Naik, J. S. Budkuley, Int. J. Nanoscience, Volume: 3, Issues: 4-5pp. 589-597, 2004.

[7] P. P. Naik, R. B. Tangsali, B. Sonaye, S. Sugur, vol. 24, pp 194-202 (2013).

[8] P. P. Naik, R. B. Tangsali, B. Sonaye, and S. Sugur, AIP Conf. Proc. 1512, 354 (2013)

[9] G. F. Goya, T.S.Berquo, F.C.Fonseca, and M P Morales, J. Appl. Phys. 94, 3520-27, (2003)

[10] Rudraji B. Tangsali Satish H. Keluskar, Ganpat K. Naik, J. S. Budkuley, J Mater Sci 42:878–882, (2007)

[11] J P Chen, C M Sorensen, K J Klabunde, G C Hadjipanayis, E Delvin and A Kostikas, Phys. Rev. B54, 9288 (1996)

[12] P. P. Naik, R. B. Tangsali, S.S.Meena , Pramod Bhatt, B. Sonaye, S. Sugur, Radiation Physics and Chemistry 102,147–152 (2014)

[13] K. Vasundhara, S. N Achary., S K Deshpande, P D Babu, S S Meena, J.Appl.Phys.113,194101(2013)

[14] U. B. Gawas, V. M. S. Verenkar, S. R. Barman, S S Meena, Pramod Bhatt, J. Alloys Compd., 555, 225–231(2013)

[15] Shalendra Kumar, A M. M Farea, Khalid Mujasam Batoo, Chan Gyu Lee, B. H Koo, Ali Alimuddin Yousef, Physica B 403, 3604–3607 (2008).

[16] D. C. Dobson, J W Linnet, M. M. Rahman, J. Phys. Chem. Solids 31,727 (1970).

[17] A. Lakshman, P.S.V Subba Rao, K. H Rao, Mater.Lett.60, 7–10, 2006.

© 2016 NSP
Natural Sciences Publishing Cor.